

# Raman Spectroscopy of Human Vitreous in Proliferative Diabetic Retinopathy

J. Sebag,\* Shuming Nie,†‡ Karen Reiser,§ M. Arthur Charles,<sup>||</sup> and Nai-Teng Yu,†¶

**Purpose.** Recent studies have demonstrated increased nonenzymatic glycation in vitreous from patients with diabetic retinopathy. The present study reports the use of Raman spectroscopy as a novel approach for investigating these molecular changes in human vitreous and experimental tissues.

**Methods.** Near-infrared laser-excited Fourier-transform (FT) Raman spectroscopy (RS) was performed on vitreous specimens obtained at surgery from seven patients with proliferative diabetic retinopathy and from 10 controls. Measurements were also obtained from samples of control and glycated (in vitro) rat tail tendon collagen and demineralized chick bone collagen.

**Results.** Spectroscopy of vitreous samples from patients with diabetic retinopathy revealed two prominent peaks at  $1604\text{ cm}^{-1}$  and  $3057\text{ cm}^{-1}$ , corresponding to aromatic C=C and C—H stretching vibrations in  $\pi$ -conjugated and aromatic molecules. The peak at  $1604\text{ cm}^{-1}$  was threefold higher in vitreous from patients with diabetes than from controls. Spectra obtained from experimental tissues provided evidence suggesting that the results obtained in human vitreous may be due to nonenzymatic glycation and not to the lysyl oxidase pathway.

**Conclusions.** These findings suggest that human vitreous obtained from subjects with diabetes may be distinguished from control vitreous by FT-RS and that the peaks characterizing the diabetic samples are possibly due to nonenzymatic glycation. Raman spectroscopy may provide a useful method to elucidate the molecular events underlying these abnormalities. Invest Ophthalmol Vis Sci. 1994;35:2976–2980.

**D** diabetes alters basement membranes and other connective tissues in virtually every organ in the body. These changes are at least in part due to an increase in early and advanced glycation,<sup>1–3</sup> phenomena that have been correlated with changes in physicochemical properties of collagen<sup>3</sup> as well as with the development of clinical complications.<sup>1</sup> Abnormalities in collagen cross-links mediated by the enzyme lysyl oxidase have also been observed in skin<sup>4</sup> and vitreous<sup>5</sup> from subjects with diabetes. There is evidence that measuring rates of change of some of these parameters, particularly nonenzymatic glycation of collagen, may have prog-

nostic value and, hence, may be useful in evaluating responses to therapy.<sup>1</sup>

In the present study, we report the application of a nondestructive technique for detailed structural analysis of tissue at the molecular level: Fourier-transform near infrared Raman spectroscopy (FT-RS). FT-RS analysis of posttranslational modifications, specifically nonenzymatic glycation and enzymatically mediated cross-linking, was performed in human vitreous and experimental animal tissues.

## MATERIALS AND METHODS

Animal investigations adhered to the ARVO guidelines for the use of animals in ophthalmic and vision research. The tenets of the Declaration of Helsinki were followed, and informed consent was obtained and signed from patients before vitreous surgery.

### Human Vitreous

Vitreous was obtained during vitrectomy surgery from seven patients with diabetes (three women, four men;

From the \*University of Southern California School of Medicine, Los Angeles; †Stanford University, Palo Alto; ‡Georgia Institute of Technology, Atlanta; the §University of California, Davis; the ||University of California, Irvine; and ¶Hong Kong University of Science and Technology, Hong Kong.

Supported by the Juvenile Diabetes Foundation International (JS); National Institute of Health grants AG05324, RR-00169, and AG07711 (KR); and by the Whitaker Foundation (SN).

Submitted for publication March 12, 1993; revised January 27, 1994; accepted January 28, 1994.

Proprietary interest category: N.

Reprint requests: Dr. J. Sebag, Pacifica Tower, 18800 Delaware Street, 11th Floor, Huntington Beach, CA 92648.

mean age,  $49 \pm 10$  years; mean duration of diabetes,  $22 \pm 7$  years) who had proliferative diabetic retinopathy (six with vitreous hemorrhage) and from 10 patients (six women, four men; mean age,  $73 \pm 7$  years) undergoing vitrectomy for retinal detachment ( $n = 5$  [2 with vitreous hemorrhage]), macular pucker ( $n = 4$ ), and vitreous hemorrhage ( $n = 1$ ). Samples were pooled into experimental (seven patients with diabetic retinopathy) and control (10 patients without diabetes) groups, then centrifuged, and the pellets were lyophilized.

### Rat Tail Tendon Collagen

Tendon fibers were removed from normal adult (4-month-old) male Sprague-Dawley rats. Tendon fibers were washed overnight at  $10^\circ\text{C}$  in 5 mM sodium phosphate buffer containing 0.9% NaCl, pH 7.4. Control tendon fibers were then lyophilized without further processing. Glycated tail tendons were prepared by incubating samples in a 2.8 M glucose solution (500 mg/ml in distilled water) containing 3 mM sodium azide at  $37^\circ\text{C}$  for 14 days in one sample and for 60 days in a second sample. The tissues were washed in distilled water five times to remove excess glucose and then lyophilized. Affinity chromatography has previously shown<sup>6</sup> that the last washing contains no free glucose.

### Demineralized Chick Bone

Bone from 7- to 8-day-old chicks was demineralized in EDTA as previously described in detail.<sup>6</sup> Chick bone normally contains the reducible cross-links dihydroxylysinoxorleucine (DHLNL) and hydroxylysinoxorleucine (HLNL), as well as the trifunctional, nonreducible cross-link hydroxypyridinium. Soluble chick bone collagen was prepared by extraction of the demineralized bone with neutral salt as previously described<sup>7</sup>; the solubilized collagen contained no detectable cross-links when aliquots of the sample were assayed by HPLC for the presence of enzymatic cross-links as previously described.<sup>7</sup> The specimens were then lyophilized.

### Raman Spectroscopy (FT-RS)

Raman spectroscopy was performed on the 10 pooled control specimens, the seven pooled diabetic specimens, rat tail tendon, and demineralized chick bone samples; all in the lyophilized state.

All FT-Raman spectra were obtained at  $4.0\text{ cm}^{-1}$  resolution using a Bruker IFS 66/FRA 106 FT-spectrophotometer (Bruker Instruments, Billerica, CA) equipped with a highly sensitive, liquid nitrogen-cooled Ge detector (Bruker). Near-IR excitation at  $1.064\ \mu\text{m}$  was provided by an Adlas diode-pumped Nd:YAG CW laser (Adlas, Stow, MA). The laser beam at the sample measured approximately 0.1 mm in di-

ameter and approximately 300 mW in power. The scattered light was collected via back-scattering geometry using an optical lens and passed through a Rayleigh light rejection filter (Bruker) into the spectrophotometer system.

Scans ( $n = 250$ ) were coadded to improve the signal-to-noise ratio. This technique has a detection limit approaching 1% (wt) for most chemical compounds. No spectral subtraction was performed in this study. The Raman spectra were normalized so that the most intense signal had a peak height of 100. For spectral analysis, we measured the peak areas, calculated as  $A = h(\text{FWHM})$ , where  $A$  = peak area,  $h$  = peak height above the baseline, and FWHM = full width at half maximum. The error of this approach is 10%. The major peaks at  $1604\text{ cm}^{-1}$  and  $3057\text{ cm}^{-1}$  were analyzed in reference to internal standards at  $1455\text{ cm}^{-1}$  and  $2930\text{ cm}^{-1}$  (C—H Raman signals) by expressing the results as ratios ( $A_{1604}:A_{1455}$  and  $A_{3057}:A_{2930}$ ). The validity of this approach has been demonstrated in previous Raman studies<sup>8,9</sup> by determining the hydration level in tissue and the contents of thiols and aromatic amino acids in proteins.

### Biochemical Assays

After Raman spectroscopy, all tissue samples (vitreous, tendon, and bone) were analyzed for the early glycation products glucitolysine and glucitolylhydroxylysine, advanced glycation endproducts, and the enzyme-mediated cross-links hydroxylysinoxorleucine (HLNL) and dihydroxylysinoxorleucine (DHLNL) as previously described in detail.<sup>4,5</sup> The human vitreous samples came from subjects who were part of a larger investigational group; results have been previously reported.<sup>5</sup>

## RESULTS

As summarized in Table 1, human vitreous specimens from these patients with diabetes had significantly higher levels of the early glycation products glucitolysine and glucitolylhydroxylysine (1.55 mol/mol collagen versus 0.48 mol/mol collagen for controls). Advanced glycation endproducts were 10- to 20-fold higher in diabetic samples than in controls.<sup>5</sup> The enzyme-mediated collagen cross-link DHLNL was significantly elevated in these diabetic samples (2.87 mol/mol collagen) than in controls (1.1 mol/mol collagen).

The FT-RS results obtained from control and diabetic vitreous specimens are shown in Figure 1. The spectra from subjects with diabetes exhibit peaks at  $888\text{ cm}^{-1}$ ,  $1251\text{ cm}^{-1}$ ,  $1604\text{ cm}^{-1}$ , and  $3057\text{ cm}^{-1}$ . The ratio of peak areas at  $1604\text{ cm}^{-1}$  compared with the internal standard at  $1455\text{ cm}^{-1}$  was 1.8 in samples from patients with diabetes. This was threefold greater than the same ratio in control samples (0.6). At  $3057$

TABLE 1. Human Vitreous Specimens

	<i>Rat Tail Tendon</i>		<i>Human Vitreous</i>	
	<i>Controls</i>	<i>14 Days' Glycation</i>	<i>Controls</i> (n = 10)	<i>Patients With Diabetes</i> (n = 7)
Collagenous lysine (%)			8.4	9.5
EGP (mol/mol collagen)	0.35	0.75	0.48	1.55
AGE (fluorometry)	2.9*	6.2*	0.3*	2.9*
	2.6†	8.6†	0.4†	7.9†
DHLNL X-links			1.1	2.87
HLNL X-links			0.41	0.49

EGP = Early glycation products (glucitolylysine plus glucitolyhydroxyllysine); AGE = advanced glycation endproducts (arbitrary fluorescence units); \* excitation at 330 nm, emission at 390 nm; † excitation at 370 nm, emission at 430 nm; DHLNL = dihydroxylysinoxidation product (mol/mol collagen); HLNL = hydroxylysinoxidation product (mol/mol collagen).

$\text{cm}^{-1}$  comparison to the internal standard at  $2930 \text{ cm}^{-1}$  yielded a ratio value = 0.1 in samples from patients with diabetes and 0.0 in controls.

Raman spectroscopic study of demineralized chick bone, which contained no DHLNL and HLNL cross-links, and of rat tail tendon (control), which contained HLNL, are shown in Figure 2. The two spectra appear essentially identical at the current signal-to-noise level. The spectra from neutral-salt insoluble chick bone, which contained both DHLNL and HLNL, was not different from soluble chick bone, which did not contain DHLNL and HLNL. It is, there-

fore, unlikely that these enzyme-mediated cross-links account for the spectral differences noted between diabetic and control vitreous samples. As shown in Figure 3, rat tail tendon glycated in vitro (14-day sample with  $0.75 \text{ mol glucitolylysine/mol collagen}$ ) had a slightly greater relative intensity at  $1604 \text{ cm}^{-1}$  than controls, consistent with the observation in human vitreous. There was also a higher relative intensity in the broad range between  $1200 \text{ cm}^{-1}$  and  $1400 \text{ cm}^{-1}$ , consistent with the aromatic ring configurations known to result from nonenzymatic glycation pathways.

We also obtained Raman spectra in the high fre-

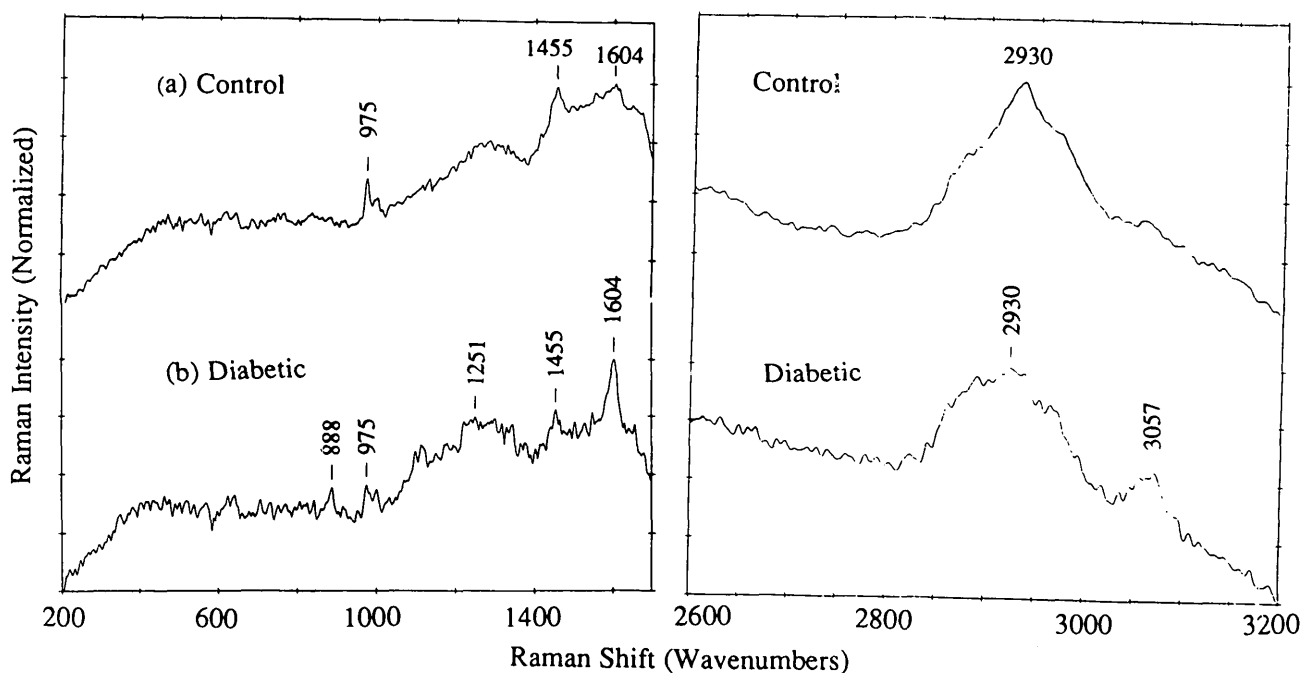
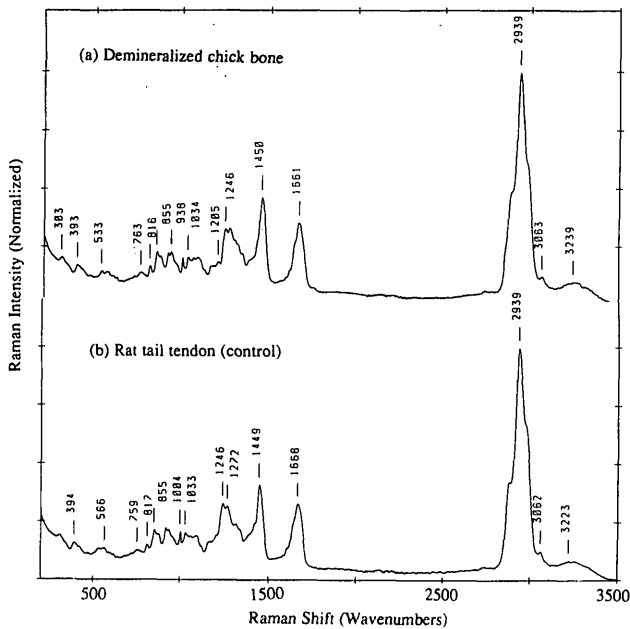


FIGURE 1. FT-Raman spectra of control and diabetic human vitreous collagen. Samples were pooled into one specimen for the patients with diabetes (n = 7) and one for the control group (n = 10). The spectra represent the actual FT-RS spectra of these two specimens. Quantitative analysis of the peak area at  $1604 \text{ cm}^{-1}$  showed a threefold increase in samples from patients with diabetes compared to controls. The broad background was corrected for when drawing the baseline of the peak at  $1455 \text{ cm}^{-1}$ . Laser power =  $300 \text{ mW}$ ; laser spot diameter =  $0.1 \text{ mm}$ ; number of coadded scans = 250.



**FIGURE 2.** Comparison of FT-Raman spectra obtained from demineralized chick bone and rat tail tendon. Laser power = 300 mW; laser spot diameter = 0.1 mm; number of coadded scans = 250.

quency region 2600 to 3500  $\text{cm}^{-1}$  for the *in vitro* glycated specimens (not shown). As for the Raman spectra in Figures 1 and 2, the following characteristic features were observed in this region: the aliphatic carbon-hydrogen (C—H) stretching signal at 2939  $\text{cm}^{-1}$ , the aromatic C—H stretching mode at 3062  $\text{cm}^{-1}$ , and the water O—H stretching mode at 3230  $\text{cm}^{-1}$ . Unlike the spectra in Figures 1 and 2, however, the aromatic O—H signal is not well resolved in the *in vitro* glycated samples, and it is difficult to derive accurate intensity information at this time. Not shown in Figure 3 are the aliphatic C—H stretching signal at 2939  $\text{cm}^{-1}$ , the aromatic C—H stretching mode at 3062  $\text{cm}^{-1}$ , and the O—H stretching mode of water at 3230  $\text{cm}^{-1}$ . In contrast to Figures 1 and 2, however, these signals were not well resolved in Figure 3, and no conclusions are drawn from this portion of the spectrum.

## DISCUSSION

Although FT-RS has previously been used in lens research,<sup>10</sup> this study represents the first characterization of the molecular effects of diabetes on human vitreous using this methodology. Protein content of vitreous specimens from a single patient was too low to perform spectral analyses on individual samples, necessitating pooling of the samples. Future studies using more sensitive spectroscopic techniques might enable individualized measurements, and, consequently,

statistical analyses would be possible. Nevertheless, the results show that substantial differences are observed in vitreous from diabetic samples, as compared to controls, confirming previous biochemical studies.<sup>5</sup> The Raman signatures in vitreous obtained from humans with diabetes demonstrate elevated peaks at 888  $\text{cm}^{-1}$ , 1251  $\text{cm}^{-1}$ , 1604  $\text{cm}^{-1}$ , and 3057  $\text{cm}^{-1}$ , as compared to controls. The interpretation of the signals at 888  $\text{cm}^{-1}$  and 1251  $\text{cm}^{-1}$  would require further experimentation not undertaken in this study. The signals observed at 1604  $\text{cm}^{-1}$  and 3057  $\text{cm}^{-1}$  are characteristic of the C=C stretching and C—H stretching vibrations in  $\pi$ -conjugated and aromatic molecules.<sup>11</sup> Advanced glycation endproducts are known to be highly complex and conjugated-aromatic molecules that act as molecular cross-links. It thus appears that the conjugated-aromatic glycation products may be selectively detected by the Raman method, primarily because these molecules are highly polarizable and have large Raman scattering cross-sections. Similarly, Raman signals at 1604 and 3057  $\text{cm}^{-1}$  are detected for

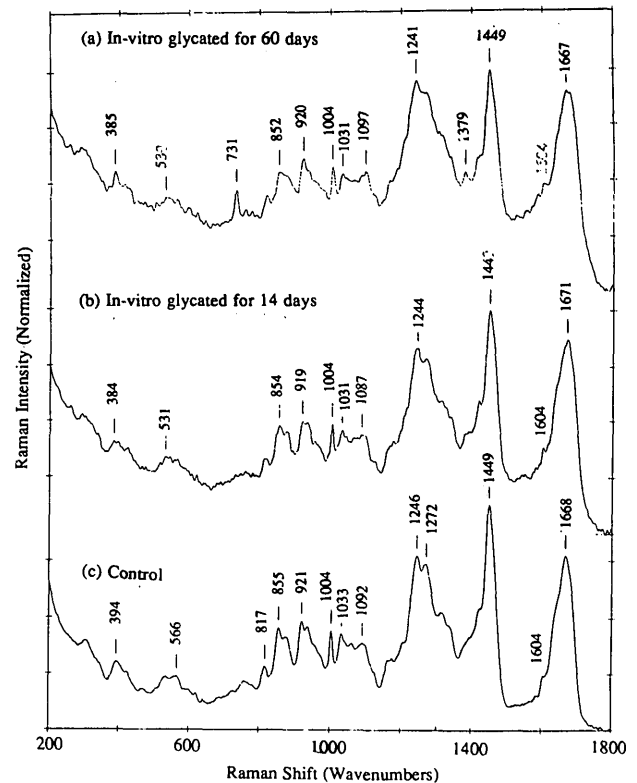


**FIGURE 3.** Comparison of FT-Raman spectra obtained from control rat tail tendon (c) and rat tail tendon glycated *in vitro* for 14 days (b) and 60 days (a). There is a slightly greater relative intensity at 1604  $\text{cm}^{-1}$  for the glycated samples (especially at 60 days) and a difference in the broad range of 1200  $\text{cm}^{-1}$  to 1400  $\text{cm}^{-1}$  with higher relative intensities in glycated samples (especially at 60 days). Laser power = 300 mW; laser spot diameter = 0.1 mm; number of coadded scans = 250.

Schiff base compounds derived from the condensation of alpha-amines and aldehydes.<sup>12</sup> It is, therefore, possible that the glycation products may also contain the Schiff base chromophore ( $—C=C—C=N—$ ). Alternatively, the peak at  $1604\text{ cm}^{-1}$  could possibly result from an olefinic CH stretch. These various possibilities could be the subject of future investigations using standard compounds and spectral modeling, as has been previously performed in human arteries afflicted by atherosclerosis.<sup>13</sup>

The results obtained from in vitro studies of rat tail tendon collagen and demineralized chick bone further suggest that the vitreous FT-RS spectra arise from nonenzymatic glycation as opposed to enzyme-mediated cross-links. Chick bone and rat tail tendon contain predominantly type I collagen, which explains why the Raman spectra from these tissues are so similar to one another and to spectra obtained from pure type I collagen. Vitreous, however, contains mostly type II collagen with lesser amounts of types V and IX.<sup>13</sup> Thus, the Raman spectra from control vitreous are not identical to those from rat tail tendon and chick bone. Nevertheless, the absence of signals at  $1604\text{ cm}^{-1}$  and  $3057\text{ cm}^{-1}$  in chick bone and the slightly increased signal at  $1604\text{ cm}^{-1}$  in glycated rat tail tendon collagen support the postulate that these findings result from nonenzymatic glycation.

It should be emphasized that the results obtained in control vitreous samples are not to be interpreted as "normal" findings because these patients underwent vitreous surgery for other vitreo-retinal pathologies,<sup>14</sup> albeit not related to diabetes. Although the control patients were older, any age-related effects would actually minimize the differences observed between the group with diabetes and the control group. Furthermore, previous studies<sup>5</sup> compared age-matched controls with patients with diabetes and found that these phenomena in younger individuals exceeded the age-related effects in the older group,<sup>15</sup> yielding significant results.

Although studies<sup>15</sup> based on fluorescent and immunologic methods have yielded important information on the molecular structure of vitreous and the phenomenon of lens protein glycation, the Raman technique provides a new means of further characterizing the molecular events underlying diabetes effects on vitreous and other connective tissues. Perhaps the greatest value of this approach lies in the theoretical potential to measure such molecular characteristics without any tissue preparation, thus possibly providing a noninvasive technique that might be used clinically to assess prognosis and to monitor the response to therapy on a molecular level.

### Key Words

diabetes, collagen, vitreous, nonenzymatic glycation, Raman spectroscopy

### References

1. Monnier VM, Vishwanat V, Frank Kay E, Elmetts Craig A, Dauchot P, Kohn RR. Relations between complications of type I diabetes mellitus and collagen-linked fluorescence. *N Engl J Med.* 1986;314:403-408.
2. Brownlee M. The role of nonenzymatic glycosylation in the pathogenesis of diabetic angiopathy. In: Draznin B, Melmed S, LeRoith D, eds. *Complications of Diabetes Mellitus.* New York: Alan R Liss; 1989:9-17.
3. Reiser KM. Nonenzymatic glycation of collagen in aging and diabetes. *Proc Soc Exp Biol Med.* 1991;37:17-29.
4. Buckingham B, Reiser K. Relationship between the content of lysyl oxidase-dependent cross-links in skin collagen, nonenzymatic glycosylation and long-term complications in type I diabetes mellitus. *J Clin Invest.* 1990;86:1046-1054.
5. Sebag J, Buckingham B, Charles MA, Reiser KM. Biochemical abnormalities in vitreous of humans with proliferative diabetic retinopathy. *Arch Ophthalmol.* 1992;110:1472-1476.
6. Reiser KM, Last JA. Analysis of collagen composition and biosynthesis by HPLC. *Liquid Chromatogr.* 1983;1:498-502.
7. Reiser KM, Amigable MA, Last JA. Non-enzymatic glycation of type I collagen—the effects of aging on preferential glycation sites. *J Biol Chem.* 1992;267:24207-24216.
8. Yu N-T, DeNagel DC, Kuck JFR Jr. Ocular lenses. In: Spiro TG, ed. *Biological Applications of Raman Spectroscopy.* Vol. 1. New York: Wiley; 1987:47-80.
9. Ozaki Y. Medical applications of raman spectroscopy. *Appl Spectrosc Rev.* 1988;24:259-312.
10. Nie S, Bergbauer KL, Kuck JFR Jr, Yu NT. Near infrared fourier transform raman spectroscopy in human lens research. *Exp Eye Res.* 1990;51:619-623.
11. Fataley W. *Characteristic Raman Frequencies of Organic Compounds.* New York: Bergman Press; 1976.
12. Bergbauer KL. *Laser Raman Spectroscopic Studies of Ocular Lens Aging and Cataractogenesis.* Atlanta, GA: Georgia Institute of Technology; 1992. Thesis.
13. Manoharan R, Baraja JJ, Feld MS, Rava RP. Quantitative histochemical analysis of human artery using raman spectroscopy. *J Photochem Photobiol.* 1992;16:211-233.
14. Sebag J. The vitreous. In: Hart W, ed. *Adler's Physiology of the Eye.* St. Louis: Mosby; 1992:268-347.
15. Araki N, Ueno N, Chakrabarti B, Morino Y, Horiuchi S. Immunochemical evidence for the presence of advanced glycation end products in human lens proteins and its positive correlation with aging. *J Biol Chem.* 1992;267:10211-10214.